Electronic Supplementary Material (ESI) for Journal of Materials Chemistry A.

Long-Term Corrosion Barrier with Insulating Boron Nitride Monolayer

Liting Shen[1†], Yuda Zhao[1,2 †], Yi Wang[1], Ruobing Song[1], Qian Yao[3], Shanshan Chen[3], and Yang Chai[1,2,]*

[1] Department of Applied Physics, The Hong Kong Polytechnic University, Hung Hom, Kowloon, Hong Kong, People's Republic of China.

[2] The Hong Kong Polytechnic University Shenzhen Research Institute, Shenzhen, People's Republic of China

[3] Department of Physics, Xiamen University, Xiamen, People's Republic of China

†Liting. Shen and Yuda. Zhao contribute equally to this work

*Correspondence should be addressed to: ychai@polyu.edu.hk, sschen@xmu.edu.cn

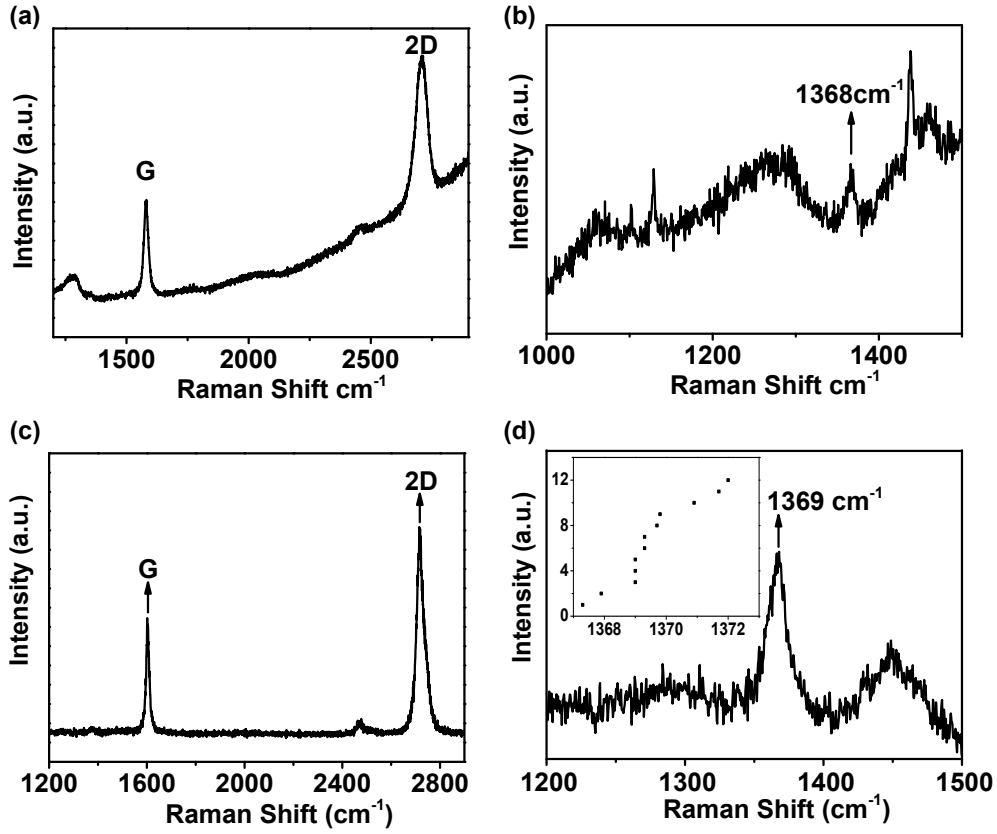

Fig. S1 Raman spectrum of (a) as-prepared graphene and (b) as-prepared BN on Cu foil. Raman spectrum of (c) graphene and (d) BN on SiO_2/Si wafer. Inset of Fig. S1d shows statistical peak positions from the 12 measurements.

The Raman peak of BN on Cu foil is very weak (See Fig. S1b). We used the PMMA-mediate method to transfer monolayer BN onto SiO_2/Si substrate. The Raman spectra of graphene and BN are shown in Fig. S1c and S1d, respectively. The peak position is around 1369±1 based on the 12 measurements, as shown in the inset of Fig. S1d. This shows that the BN is mainly monolayer.[1]

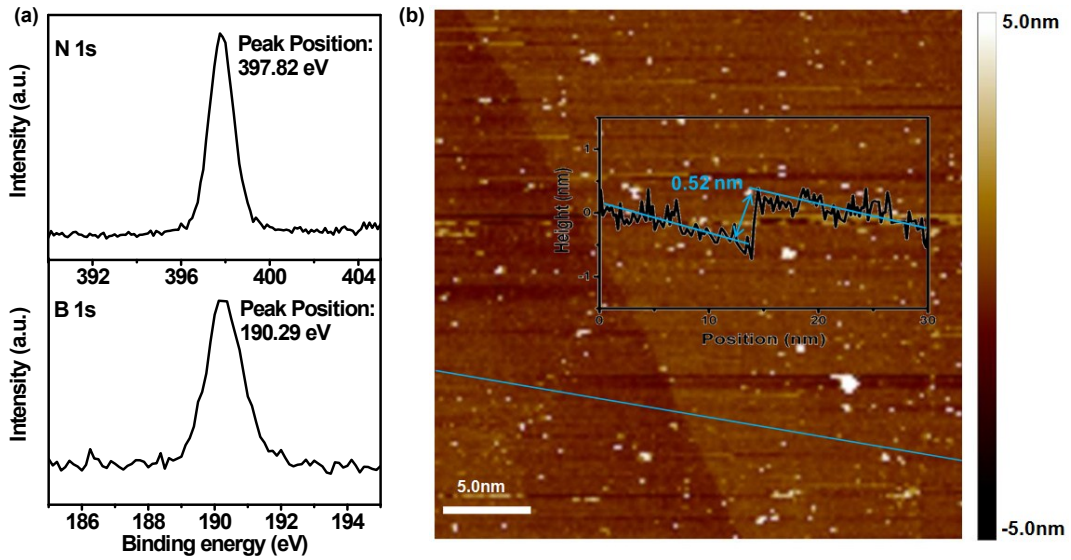

Fig. S2 (a) XPS spectrum of the N1s electrons and B1s electrons. The peak positions are 397.8 eV and 190.3 eV, respectively. The N to B ratio is around 1.07, showing that the material is mainly BN (b) AFM image of the BN layer. The thickness is around 0.52 nm, corresponding to the monolayer BN.

We experimentally verified the existence of BN on copper foil by XPS characterization. In Fig. S2a, a peak around 397.8 eV is exhibited, corresponding to the N 1s electron peak.[1] The B 1s electron peak is detected with a binding energy of 190.3 eV, which is in good agreement with the results reported by Kim *et al.*[1] The XPS data show that the N/B ratio is around 1.07, which close to the result of (55:45) by Kim *et al*[1] and the result of (1.12:1) by Shi *et al*[2].The relative higher atomic percentage of N atoms indicates that the major defects in the BN layer are B defects.

We conducted AFM characterization to accurately measure the thickness of BN layer. Fig. S2b shows the AFM image of BN on Si substrate. The thickness of BN is measured to be less than 0.52 nm, which is close to the monolayer BN thickness (0.42 nm) reported by Kim *et al.* and the monolayer value in bulk crystal (0.33 nm).[1,3] The difference can be caused by the BN transfer process and the adsorbed molecules on the substrate. It shows that the BN in this work is mainly monolayer.

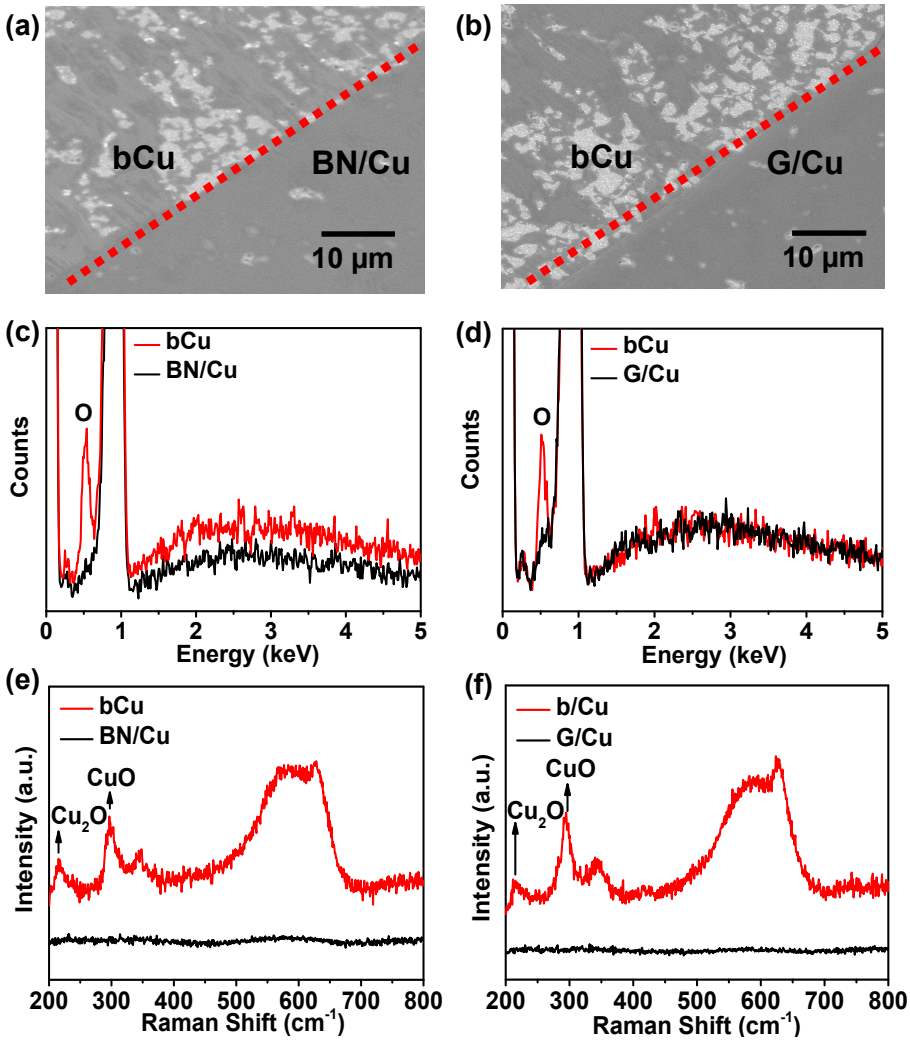

Fig. S3 SEM images of the partially protected Cu foil dipped in HNO_3. Note that the parts with (a) BN and (b) graphene are protected. EDS analysis performed on the two regions of partially coated with (c) BN and (d) graphene. (e) Raman spectra of the Cu foil partially coated with (e) BN and (f) graphene.

Fig. S3a and S3b are the images of partially protected Cu foil after acid corrosion. The samples were dipped in HNO_3 (1.0 M) solution for around 15 minutes. Significant morphology difference in bCu (Cu foil) and BN/Cu sections can be observed in Fig. S3a. The bCu section is severely oxidized after the corrosion. Similar contrast can be observed between the G/Cu and bCu sections in Fig. S3b. We performed energy dispersive X-ray spectroscopy (EDS) characterization to quantitatively study the protection effect of BN and G monolayers. For the BN/Cu section, the O percentage is around 2.37%, almost 14% of the unprotected section (Fig. S3c). For the G/Cu region, the O percentage is about 3.12%, around 17% of the bCu region (Fig. S3d). It shows that BN and G effectively prohibit the corrosion of Cu under acidic solution.

We also performed Raman characterization to determine the oxidized contents. As shown in Fig. S3e and S3f, for the bare samples, single peaks are present at around 218 cm^{-1} and 300 cm^{-1} corresponding to Cu_2O[4] and CuO[5] contents, respectively. However, negligible peaks can be observed for the BN/Cu or G/Cu regions. The strong spectroscopic contrast also supports that the BN and G can effectively protect Cu under acidic environment. Different from what we observed in the long-term corrosion spectrum, where the two Cu_2O peaks are much greater than that of the CuO peaks, the CuO peak has higher intensity than Cu_2O in short-term and intensive corrosion. This indicates that the corrosion content mainly consists of CuO instead of Cu_2O.

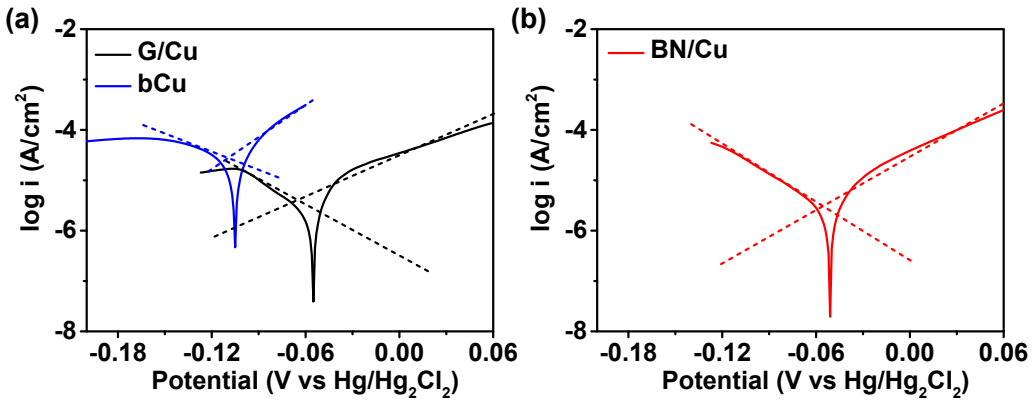

Fig. S4 Extrapolation method applied on Tafel plot of the bCu, G/Cu, and BN/Cu samples.

We found that the equilbrium potential (E_{eq}) shifts to the positive direction by around 50 mV. This can be explained by the increase of copper concentration. We introduce the Nernst half-cell equations to explain the equilibrium potential shifts:

$$E_{eq} = E_{eq}^{0} + \frac{59}{m}\log\left(a_{ions}\right) \qquad \text{(S. 1)}$$

E_{eq} is the equilibrium potential and m is the valence number 2 for Cu^{2+} and 1 for Cu^{1+}. a_{ions} is the activity of Cu ions. According to equation (S.1), the potential of calomel reference electrode in 0.1 M Cl^- environment is around 334 mv. All the value of voltages in this calculation are voltage with reference to standard hydrogen electrode (SHE). For copper oxidation, we take E_{eq} as +284 mv for coated samples, E_{eq}^{0} as +342 mv (Cu^{2+}) and valence number as 2. We use the same method to calculate the activity

cupric ions of the uncoated copper. It is found that the activity of protected copper is 50 times as much as that of the uncoated copper.

Table S1 Impedance data of the three samples are fitted to the equivalent circuit model (Randles-Warburg model).

	R_s (kΩ)	R_{ct} (kΩ/cm^2)	y_o for CPE ($\times10^{-5}$ $\Omega^{-1}s^n$/cm^2)	n	C_{dl} (μF/cm^2)	y_o for W ($\times10^{-5}$ $\Omega^{-1}s^{1/2}$/cm^2)
G/Cu	4.60	175	2.40	0.77	17	5.07
BN/Cu	4.67	279	0.740	0.82	3.3	5.76
b/Cu	4.54	77.1	7.00	0.80	53	54.0

The impedance data is analyzed using the Randles-Warburg model. The model is characterized by R_s, R_{ct}, Z_{CPE}, Z_w, and C_{dl}. Z_{CPE} is given by $Z_{CPE}=(j\omega)^{-n}\ y_o^{-1}$, where j is the imaginary unit, ω is the angular frequency of the voltage and y_o for CPE and n is calculated using Zview software. C_{dl} can be calculated by $C_{dl} = y_o(\omega_{max})^{n-1}$, where ω_{max} is the frequency where the imaginary part of the impedance is maximized and y_o and n are parameters characterizing Z_{CPE}. The impedance of Warburg element is estimated using the formula $Z_w=(j\omega)^{-0.5}\ y_o^{-1}$, where j is the imaginary unit, ω is the angular frequency of the voltage and y_o for W is calculated using Zview software.

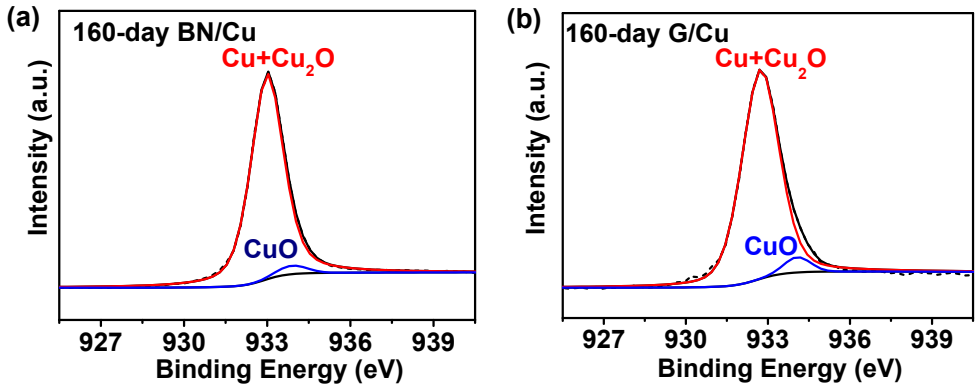

Fig. S5 The $Cu2p_{3/2}$ electron spectrum of (a) BN/Cu and (b) G/Cu. The deconvolution methods show that the Cu(II) content is 1.3% and 4.3% in BN/Cu and G/Cu sample, respectively.

The XPS spectrum on G/Cu has a larger CuO peak than the spectrum of BN/Cu after deconvolution. The percentage of the Cu(II) content in G/Cu is 4.3%, three times as much as that of the BN/Cu sample (1.3%). The $Cu2p_{3/2}$ peaks are located at 932.9 eV and 933.0 eV in Fig. S5a and S5b, respectively.

References:

1. K. K. Kim, A. Hsu, X. Jia, S. M. Kim, Y. Shi, M. Hofmann, D. Nezich, J. F. Rodriguez-Nieva, M. Dresselhaus, T. Palacios and J. Kong, *Nano Lett.*, 2012, **12**, 161-166.

2. Y. M. Shi, C. Hamsen, X. T. Jia, K. K. Kim, A. Reina, M. Hofmann, A. L. Hsu, K. Zhang, H. N. Li, Z. Y. Juang, M. S. Dresselhaus, L. J. Li and J. Kong, *Nano Lett.*, 2010, **10**, 4134-4139.

3. A. Nag, K. Raidongia, K. Hembram, R. Datta, U. V. Waghmare and C. N. R. Rao, *ACS Nano*, 2010, **4**, 1539-1544.

4. H. Gao, J. Zhang, M. Li, K. Liu, D. Guo and Y. Zhang, *Curr. Appl. Phys.*, 2013, **13**, 935-939.

5. M. H. Chou, S. B. Liu, C. Y. Huang, S. Y. Wu and C. L. Cheng, *Appl. Surf. Sci.*, 2008, **254**, 7539-7543.